Impact of monovalent metal halides on the structural and photophysical properties of halide perovskite

Mojtaba Abdi-Jalebi[1*], M. Ibrahim Dar[2]

[1] Institute for Material Discovery, University College London, Torrington Place, London WC1E 7JE, UK

[2] Cavendish Laboratory, Department of Physics, University of Cambridge, JJ Thomson Avenue, Cambridge CB3 0HE, UK

*Email: m.jalebi@ucl.ac.uk

Abstract

In this chapter, we discuss the importance and impact of addition of metal halide additives into perovskite to enhance its semiconductor quality and realize highly efficient and stable perovskite photovoltaic devices. Monovalent metal halides have been introduced as the most promising candidates due to the their loading capacity and chemical compatibility with the perovskite materials as well as ease of incorporation and their remarkable positive impact on the crystal growth, optoelectronic properties and subsequently the performance of perovskite solar cells (PSCs). Among all the monovalent metal cations, Cs is the only one that could fit in the perovskite structure and forms photoactive perovskite and the other monovalent cations are located at the interstitials sites, grain boundaries and crystalline surfaces. We also discuss the key roles of monovalent metal halide additives that includes modulating morphology of perovskite films, modification of structural and optoelectronic properties, adjusting energy level alignment in PSCs, inhibiting non-radiative recombination in perovskites, eliminating hysteresis and enhancing operational stability of PSCs.

Keywords

Monovalent metal halide; Additives; Alkali metal cations; Optoelectronic properties; Photovoltaic parameters; Solar cell efficiency

Table of Contents

1. Introduction

Additive engineering have been a key enabler to tune and optimise material and optoelectronic properties of metal halide perovskites to enhance their performance and stability in various applications such as solar cells[1,2] and light emitting diodes[3,4] (LEDs), field-effect transistors[5] and X-ray detectors[6]. These properties including morphology, crystallinity, trap-state density and luminescence efficiency have a direct impact on the performance of perovskite devices[7]. Halide perovskites are remarkably tolerant to additives due to its unique crystal and band structure which provides a wide range of creative space for additive engineering[8]. The main two category of additives includes inorganic adjunct (e.g. metal halides[9,10], nanoparticles[11] and inorganic acids[12]) and organic additives (e.g. small molecules[13], ionic liquids[14], polymers[15] and fullerenes[16]). The latter is less prominent since its limited impact on surface states whereas the density of traps in the bulk is prominent. Furthermore, the organic elements in halide perovskites is shown to be the source of instability and adding organic adjunct could potentially impact negatively on the long-term stability of perovskite devices[17]. Subsequently, the inorganic additives in particular metal cations have been introduced as the key influencers on both surfaces and the bulk of the halide perovskites to enhance their structural and optoelectronic properties.

2. Metal halides

Upon addition of metal halides into the perovskite system with ABX_3 formula, the metal cation could directly impact on the A- or B- sites based on the ionic radius and its valence and the halide will be incorporated in X site. Thus far, various metal cations with a wide range of ionic radius have been added to the perovskite systems (Figure 1a). Notably, the metal cations could be either incorporated into the perovskite structure or located at the crystalline surfaces such as grain boundaries and interfaces. The incorporation of the metal cations could be in the form of doping[18,19] (e.g. interstitial or substitutional) or formation of alloyed structures[20,21]. It is notable that most of the metal cations are mismatched to sustain a photoactive ABX_3 perovskite with an appropriate Goldschmidt tolerance factor between 0.8 and 1.0 and therefore does not form the alloyed structures (Figure 1b)[22]. The metal halide additives are usually categorise into monovalent[9], divalent[23,24] and trivalent[19] cation halides based on the nature of the metal cation. The monovalent metal halides are the most common type of metal halide additives and we will discuss their impact on the structural and optoelectronic properties of perovskite materials in the following sections.

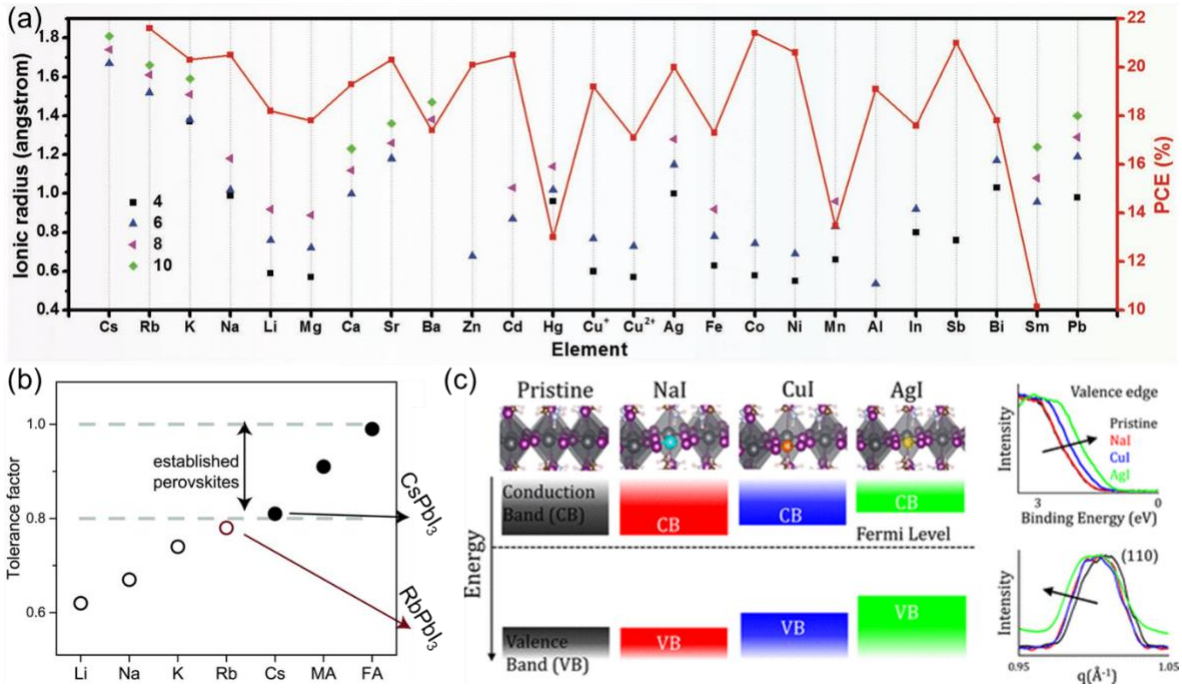

Figure 1. Incorporation of metal halide additives in perovskites. (a) The ionic radius for a range of cations with different coordination numbers versus the highest achieved PCE of the perovskite solar cells with metal cation additives[25]. (b) Tolerance factor of $APbI_3$ perovskite with the oxidation-stable A (Li, Na, K, Rb, or Cs) and MA or FA. The dashed lines (tolerance factor between 0.8 and 1.0) represent the range for formation of perovskite with photoactive black phase (solid circles) compare to nonphotoactive phases (open circles)[22]. (c) Schematic representation of the valence and conduction band edges position *vs* the Fermi level (black dot line) induced by the incorporation of monovalent metal halides. The two plots on the right show the position of valence band edge and the main perovskite diffraction peak (110) of pristine and perovskite thin films with monovalent metal halides[26].

3. Monovalent metal halides

This category of the metal halide additives includes alkali metal cations[27] and a number of transition metals such as silver[28] and copper[9,29]. Among various monovalent cations, the ionic radius of cesium and rubidium are closer to the A- site while the ionic radius of sodium and silver are the closest match to the B- cite (e.g. Pb). Although the other monovalent metal cations's ionic radius (e.g. Li, Cu) would not match neither A- site nor B- site, they have been used as the surface modifiers or locating at the interstitial site within the perovskite crystal structures[30].

Cesium is the most common monovalent cation that could fit within the A- site in ABX_3 perovskite structure as well as forming alloyed compositions with the most common organic A- site cation such as MA = methylammonium, $CH_3NH_3^+$ and FA = formamidinium,

$CH_3(NH_2)_2^+$) as all these cations are placed within the appropriate range of Goldschmidt tolerance factor (i.e. 0.8 and 1.0) and form black α-phase perovskite[20]. It is notable that Cs was first introduced in the perovskite system to inhibit the undesired phase transition and anhance the photo- and moisture stability of the FA based perovskites via shrinkage of cubo-octahedral volume and stronger chemical interaction between FA and iodine that lead to reduction in trap density and ionic migration[31]. Particularly, a combination of Cs with FA and MA where FA is the dominant cation known as alloyed triple action perovskite (e.g. $(Cs_{0.06}FA_{0.79}MA_{0.15})Pb(I_{0.85}Br_{0.15})_3$) become the state of the art composition in the field since it is thermally more stable, contain less phase impurities and are less sensitive to processing conditions[20,32].

The implementation of monovalent metal halide started in 2016 by Abdi-Jalebi et al via addition of Cu, Na and Ag with similar ionic radii to Pb into the $MAPbI_3$ to explore the possibility of doping in this system[9]. These monovalent cations remarkably impact the structural and optoelectronic properties and alter the electronic band structure of the perovskites (Figure 1c)[26]. This studies followed by other works and particularly the addition of Rb in the complex composition of triple cation perovskites enhance power conversion efficiency (PCE), thermal and photostability that is attributed to the enlarged grain size with the reduced non-radiative recombination and entropic gains through a unique defect passivation mechanism[22]. The next breakthrough in the field happened through addition of potassium into the alloyed triple cation perovskite system that leads to inhibition of ionic migration and formation of Frenkel defects that leads to significant bandgap stability in mixed halide perovskite systems across a wide range of bandgap (e.g. 1.7 to 1.9 eV) and the complete removal of hysteresis in perovskite solar cells[30,33]. The mechanism of enhancement with potassium halide additives includes decoration of the surface and grain boundaries with potassium while filling the halide vacancy with the excess halide from KI[34]. Due to the sequestration of K, excess halide is immobilized at the grain boundaries and surfaces, thereby inhibiting halide migration in parallel with suppressing hysteresis and photo-induced ion segregation[34]. All the monovalent metal cation halide have been shown to be beneficial for the grain growth[35] and formation of uniform pin-hole free perovskite thin films with larger grains that in turn lead to higher optoelectronic performance and stability in the subsequent devices[25].

4. Impact of monovalent metal halides on the morphological, structural and optoelectronic properties of perovskites

The addition of monovalent metal cation halides to the perovskite materials have been reported extensively though the composition of the perovskites in these studies were different and evolve over time from single cation (e.g. $MAPbI_3$, $FAPbI_3$)[9,36] to more complex composition such mixed cation lead mixed halide perovskite[22,33,37]. Thus, it is imperative to discuss and compare the influences of monovalent metal cations on identical perovskites to obtain an optimal matching. In most of the perovskite systems, these additives alter the grain growth and morphology of the perovskites as shown in Figure 2. Although there is no general trend for all of these cations, the increase in the average size of the grains, higher uniformity and smoothness with better surface coverage and removal of the pin-holes are the common enhancement observations in the morphology of the perovskite thin films after addition of these additives (Figure 2). These enhancements in the film quality of perovskites upon addition of the additives mostly attributed to the controlled crystal growth of perovskite thin films[9,38]. It is notable that the formation of larger grains in perovskite thin films is favourable for the optoelectronic performance of the subsequent devices as the density of the grain boundaries that are known as the main source of non-radiative recombination centres will significantly diminish upon increasing the grain size[39].

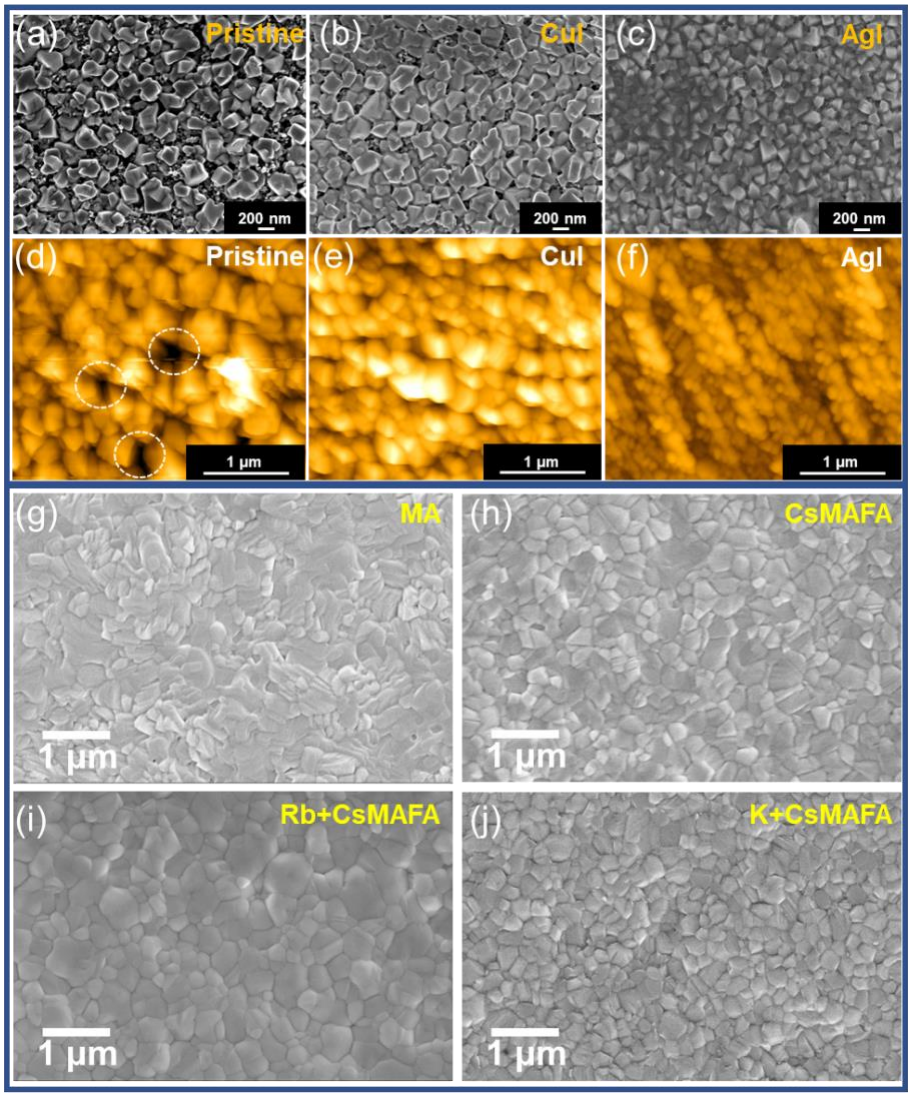

Figure 2. Morphological modifications of perovskites with monovalent metal halides. Top-view scanning electron microscopy (SEM) and atomic force microscopy (AFM) images of (a, d) pristine, (b, e) CuI-, (c, f) AgI-based $MAPbI_3$ deposited on a mesoporous TiO_2-coated fluorine-doped tin oxide (FTO) glass by two-step sequential spin-coating[9]. SEM images of (g) MA-, (h) CsMAFA-, (i)Rb+CsMAFA-, and (j) K+CsMAFA-based lead mixed halides ($APb(I_{0.85}Br_{0.15})$ deposited on FTO coated glass via single step anti solvent spin-coating[32].

The monovalent metal halide additives plays effective roles in defining the structural properties such as the average crystalline size, crystalline phase, lattice constant and crystal orientation of the perovskite materials (Figure 1c and Figure 3)[36]. In particular, one of the key method to ensure the complete conversion of PbI_2 into perovskite in the conventional sequential two-step deposition technique is the disappearance of the corresponding PbI_2 feature in the X-ray diffraction spectra[40]. For instance, the addition of NaI leads to complete conversion of lead iodide into $MAPbI_3$ perovskite evidenced by the vanished diffraction peak of PbI_2 as shown in

Figure 3a. Interestingly, in the complex composition of mixed cation lead mixed halide with excess lead iodide, addition of potassium reduces the amount of PbI_2 residue where at higher concentration of potassium (e.g. x=0.40), the PbI_2 peak has completely vanished and a new phase which is reach in potassium appears and become stronger at higher concentration of potassium (Figure 4). It is shown that the addition of monovalent metal cation such Li, Na and K increase the lattice constant of the perovskite however the larger cations such as Rb and Cs has not impact on the lattice parameter (Figure 3b). Taking into account the ionic radius and tolerance factor, the Rb and Cs are capable to be settled down on the A site while the Li, Na and K are difficult to occupy the A site.

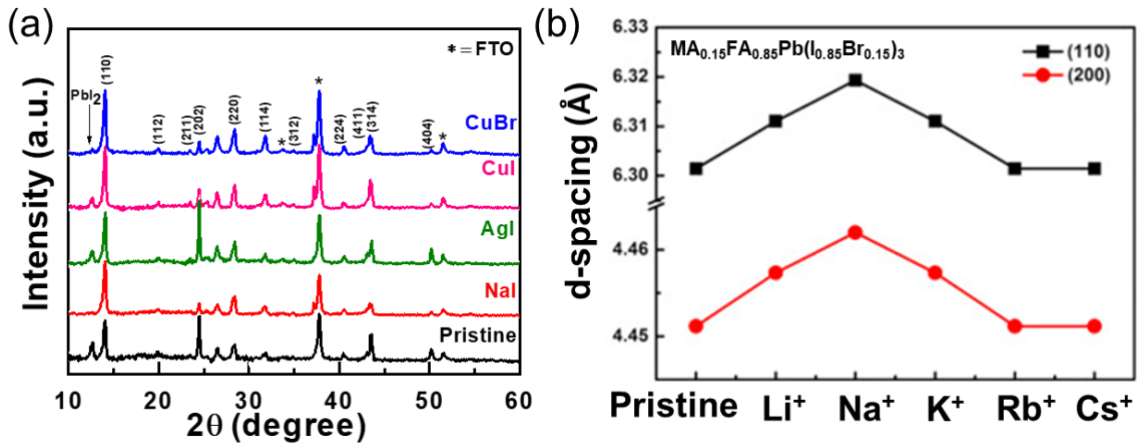

Figure 3. Impact of monovalent metal halides additives on the structural properties of perovskites. (a) X-ray diffraction spectra of pristine and $CH_3NH_3PbI_3$ perovskite with metal halide additives that is grown on mesoporous TiO_2 film which is deposited on the FTO-coated glass[9]. (b) The d-spacing of alkali cations incorporated-$MA_{0.15}FA_{0.85}Pb(I_{0.85}Br_{0.15})_3$[41].

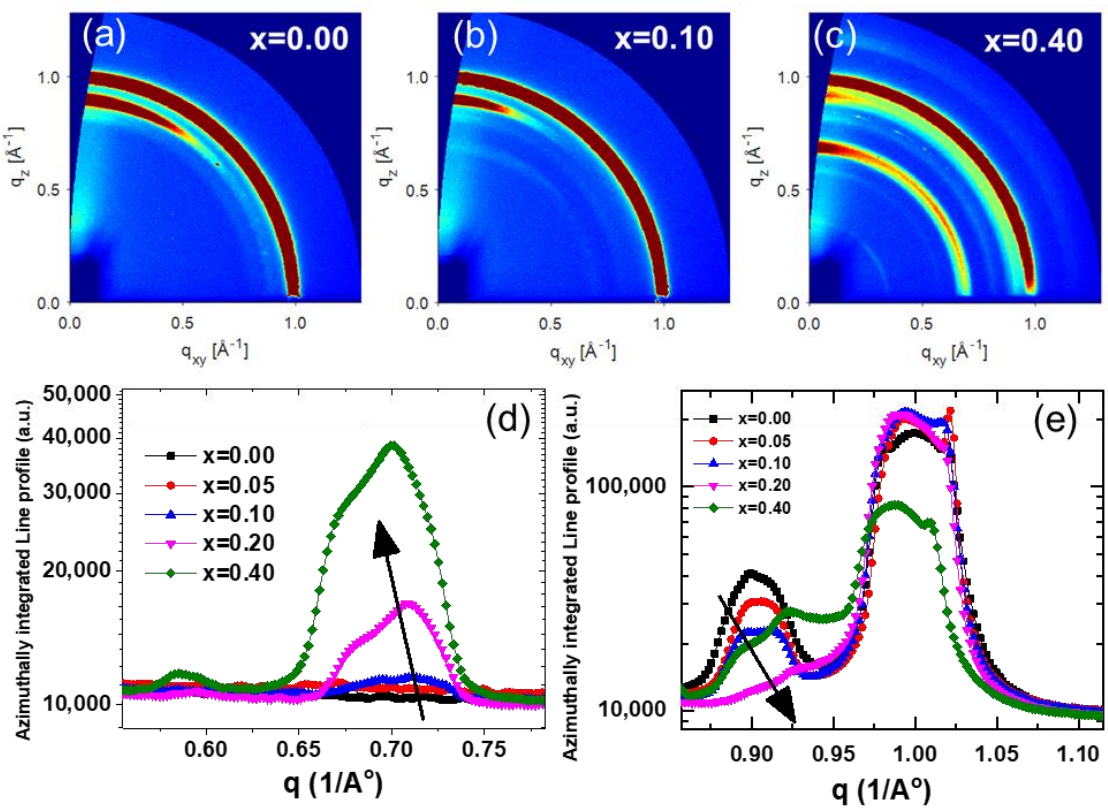

Figure 4. Impact of potassium iodide addition on the crystal structure of triple cation lead mixed halides ((Cs,FA,MA)Pb($I_{0.85}Br_{0.15}$)$_3$). The diffraction patterns of thin (Cs,FA,MA)Pb($I_{0.85}Br_{0.15}$)$_3$ films collected at low angle using GIWAXS for (a) x=0.00, (b) x=0.10, and (c) x=0.40. (d, e) The high-resolution line profiles azimuthally integrated over the entire GIWAX profile for different fractions of potassium at 0.5≤q≤0.8 (d) and 0.8≤q≤1.1 (e)[33].

Notably, the location of these monovalent metal cations excluding cesium that fits well within the A-site in the perovskite crystal structure are still under debates though interstitials sites[42], grain boundaries[33] and crystalline surfaces[9] are the plausible locations. On this front, scanning transmission electron microscopy energy dispersive X-ray spectroscopy (STEM-EDX) together with a Non-negative Matrix Factorization (NMF) algorithm[43] and hard-X-ray photoelectron spectroscopy (HAXPES)[26,44] were the two key advanced techniques that were used to locate these cations. Utilising STEM-EDX with NMF analysis, various compositional phases were observed for the potassium- and rubidium-passivated mixed cation lead mixed halides systems that includes a monovalent cation halide additive-rich phase and a perovskite phase (Figure 5a-f). In the alloyed perovskite systems with potassium addition, the K-(additive)-rich phase is composed of K and Br and situated at the grain boundaries and interfaces of the perovskite film[33]. However, addition of rubidium in the same system with

identical concentration, forms large, mixron sized crystals rich in Rb and iodide (Figure d-f)[44]. To get a deeper insight into the chemical composition, distribution, and electronic structure of the perovskite films with monovalent metal cation halide additives at the surface and bulk, soft X-ray photoelectron spectroscopy (XPS, 1486.6 eV photon energy) and synchrotron HAXPES (4000 eV photon energy) were utilized[26]. These measurements in the alloyed perovskite systems with potassium and rubidium halide additives reveal that Rb is more uniformly distributed throughout the film, with a negligible change when probing the surface (XPS) and probing deeper into the bulk (via the use of hard X-rays, HAXPES); on the other hand, the K content is higher on the surface than that in the bulk (Figure 5g-j).

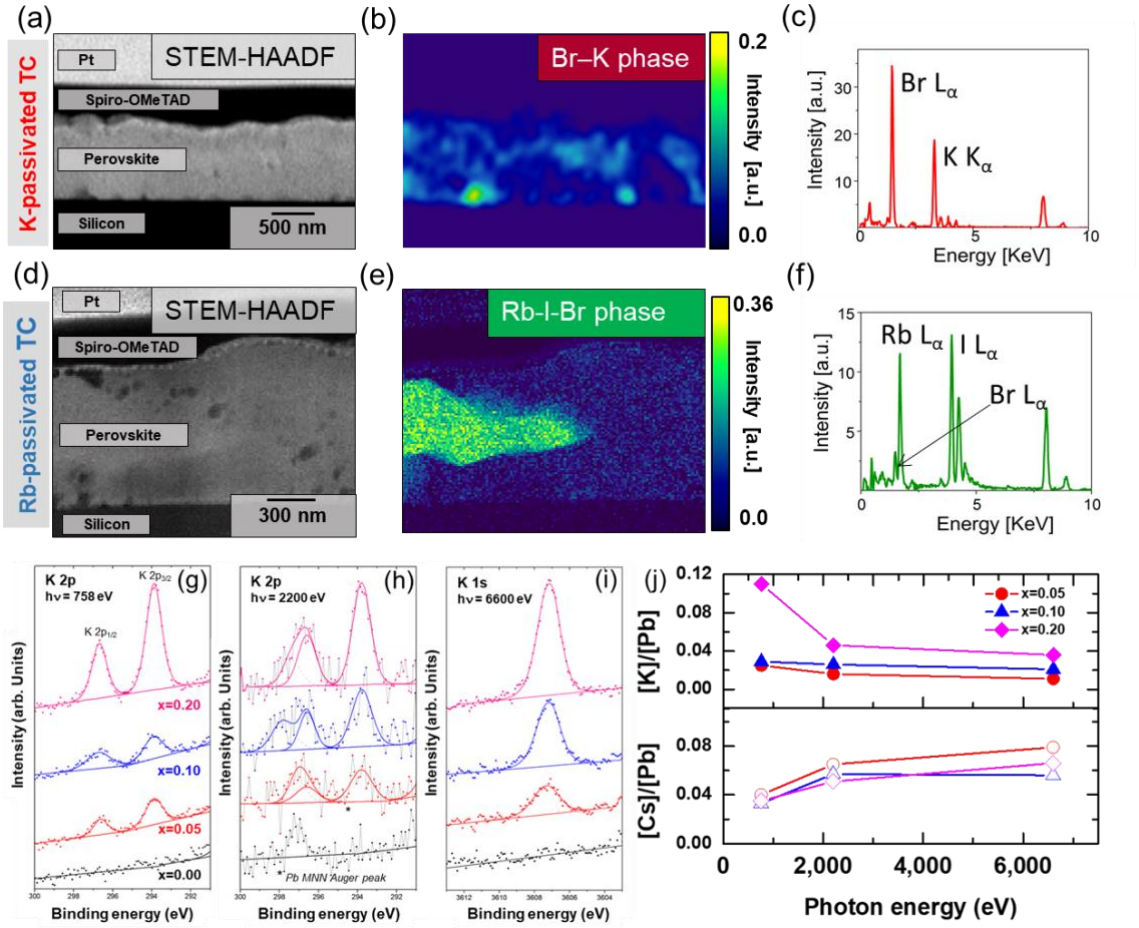

Figure 5. Locating the monovalent metal halide additives in perovskite thin films with STEM-EDX and HAXPES. (a) HAADF STEM cross-sectional image of a triple cation alloyed perovskite thin film potassium addition (x = 0.10). (b) NMF decomposition of this potassium-based perovskite showing the KBr phase and (c) the corresponding EDX spectra. (d) HAADF STEM cross-sectional image of a Rb-based perovskite (x = 0.10). (e) NMF decomposition of the Rb-based perovskite showing the Rb–I–Br phase and (f) the

corresponding EDX spectra[44]. The HAXPES spectra of the K-based perovskite films for 2P and 1S core levels recorded with a photon energy of (g) 1486.6 eV, (h) 2200 eV and (i) 6600 eV. (j) Intensity ratio between core levels ([Cs]/[Pb] and [K]/[Pb]) calculated from the experimental results as a function of photon energy (measurements at 758, 2,200 and 6,600eV) [33].

In addition to the growth mechanism, morphology and structure of halide perovskites, their optoelectronic properties remarkably enhanced via addition of optimised amount of monovalent metal cation halide into the system. Although the bandgap and emission peak of the perovskite from the absorption and photoluminescence spectra, respectively, have not been affected remarkably via addition of these additives, the charge career lifetime and photoluminescence quantum yield (PLQE) enhanced significantly. For instance, addition of Na, Cu and Ag in the MAPbI3 perovskites increased the PLQE (from less 5% to about 20% for Na addition) and diminished the urbach energy (i.e. sharper bandedge) that is representative of the energetic disorder in the semiconductor. The enhanced PLQE and PL lifetime collectively suggest that these monovalent metal cation additives are able to eliminate non-radiative decay channels in the perovskite thin films and achieve long carrier lifetime.

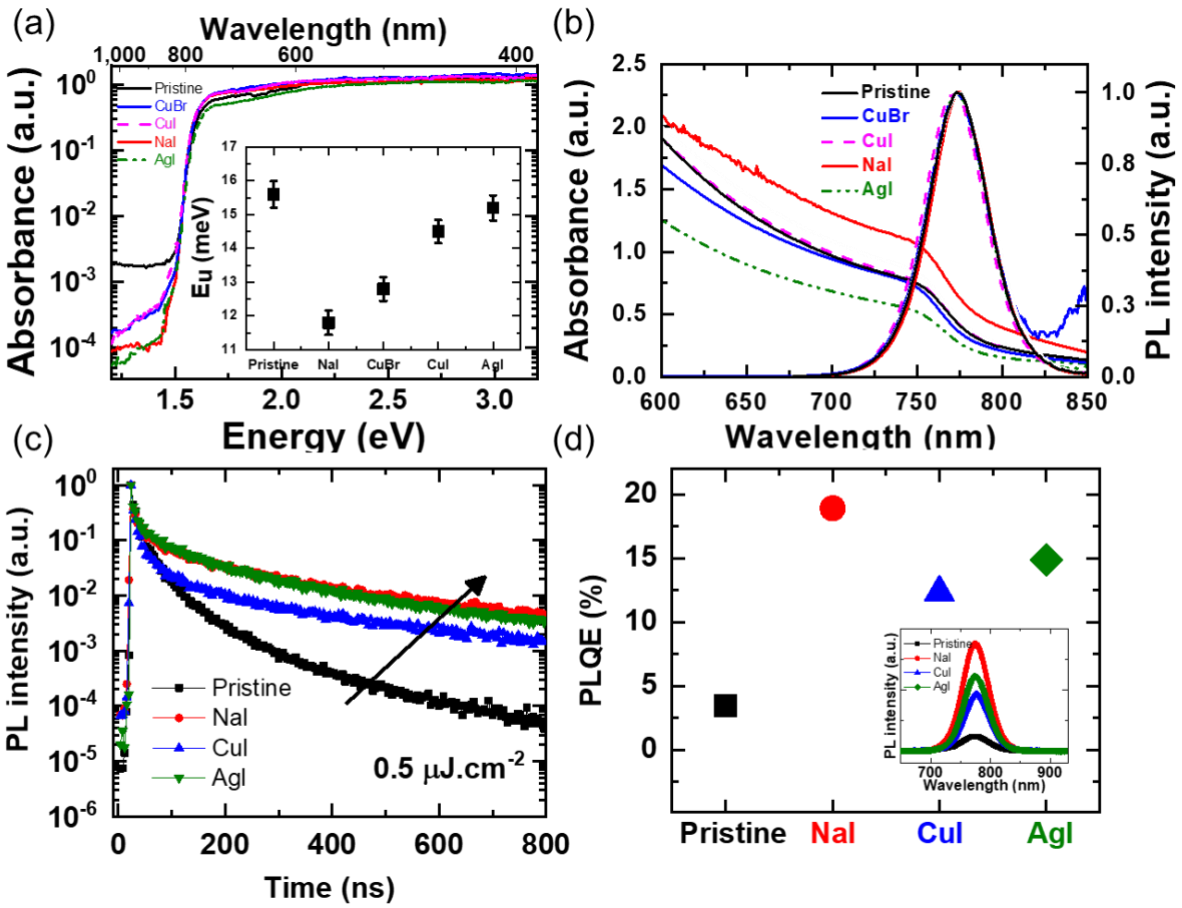

Figure 6. Enhanced optoelectronic quality of perovskite thin film via addition of monovalent cation halides. (a) The photothermal deflection spectroscopy absorption spectra of perovskite films derived from pristine and monovalent metal halide additive based perovskites measured. The inset shows the corresponding Urbach energies for all samples. (b) Steady-state absorption and photoluminescence spectra for pristine and additives based perovskite films.[9] (c) Time-resolved PL decays of the doped perovskite films, with excitation at 400 nm and a pulse fluence of 0.5 μJ cm^{-2}. (d) PLQE of the doped perovskite films measured under illumination with a 532 nm laser. The inset shows the PL spectrum of the pristine and doped perovskite films[26].

It is notable that for a solar cell or light-emitting diode to approach its efficiency limit, all recombination should be radiative and the luminescence should be maximized[33]. Addition of monovalent metal cation halides in particular potassium iodide have been the most effective approach to supress the substantial non-radiative losses that originate from charge-carrier trap states present in the state-of-the-art perovskite films[45–47]. The alloyed perovskite film with potassium iodide additives reached a very high stable PLQE of 66% over time (Figure 7a) as well as at different excitation power (Figure 7b) that confirms the substantial removal of the

non-radiative losses within the perovskite[33]. This finding are also observed in micro-photoluminescence maps of the perovskite films acquired by confocal photoluminescence microscopy that shows the continuous enactment of emission intensity at higher concentration of potassium (Figure d-f)[33]. The remarkable increases in luminescence efficiency of alloyed perovskite film with addition of potassium compare to other monovalent metal cation such as Rb attributed to the tolerance of these perovskites for higher loadings of K than Rb (Figure 7c)[44].

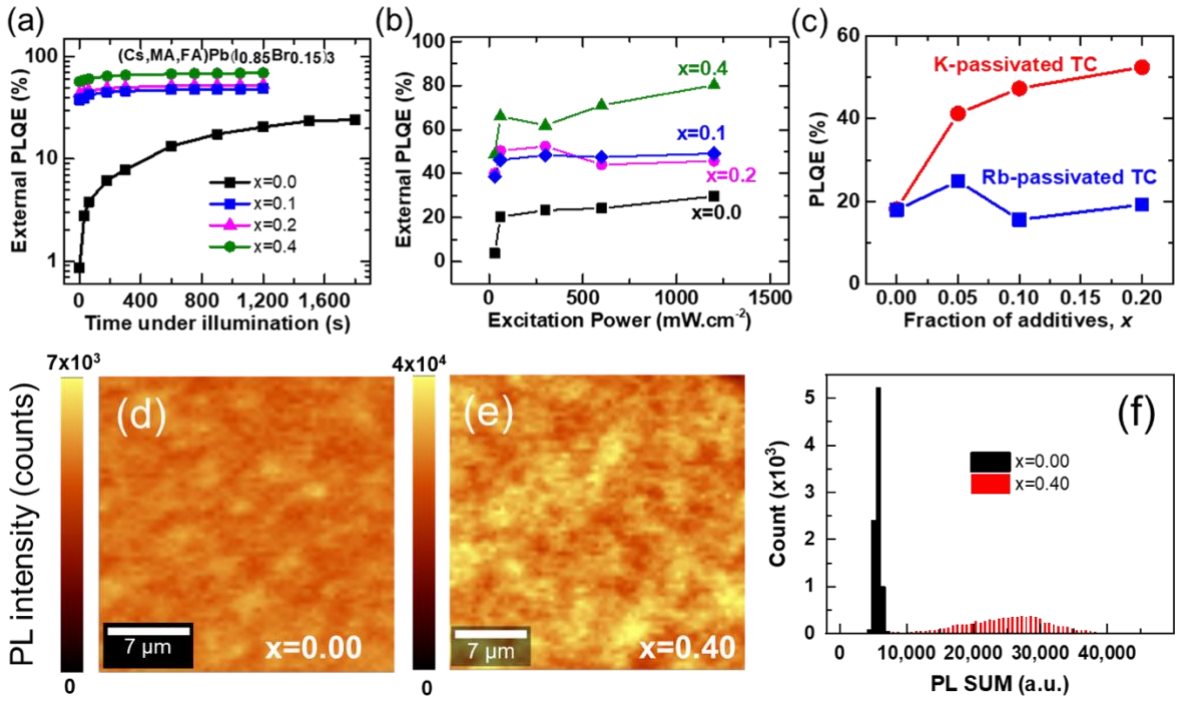

Figure 7. Increased radiative efficiency of perovskite thin films via addition of monovalent metal halides. (a) PLQE time course for (Cs,FA,MA)Pb($I_{0.85}Br_{0.15}$)$_3$ films with different fraction of potassium illuminated with a 532-nm laser at an excitation intensity equivalent to approximately 1 sun (60mWcm^{-2}) in an ambient atmosphere. (b) PLQE as a function of excitation power measured by a 532-nm continuous-wave laser for potassium-based perovskite thin films in an ambient atmosphere. (c) PLQE of K- and Rb-based perovskite thin films measured under illumination with a 532 nm laser at an excitation intensity equivalent to ~1 sun (~60 mW·cm^{-2})[44]. Confocal photoluminescence intensity maps with 405-nm excitation measured in ambient atmosphere for (Cs,FA,MA)Pb($I_{0.85}Br_{0.15}$)$_3$ perovskite thin films with (d) x=0.0 and (e) x=0.40 fraction of potassium. (f) Histograms of the absolute photoluminescence intensities extracted from the respective maps for x=0 and x=0.40[33].

5. Impact of monovalent metal halides on photovoltaic device characterizations

The power conversion efficiency (PCE) of the solar cell is subservient to the photophysical properties of the light absorber layer, which in turn depend on the compositional, structural, and morphological properties of the perovskite layer, thus collectively determine the output power (P_{out}), and stability. The P_{out} of a solar cell is the product of three photovoltaic parameters, including short-circuit photocurrent density (J_{SC}), open-circuit voltage (V_{OC}) and fill factor (FF) divided by the input power (P_{in}) (equation 1).

$$Pout = \frac{J_{sc} \cdot V_{oc} \cdot FF}{P_{in}} \qquad (1)$$

To realize maximum P_{out}, all the three photovoltaic parameters need to improved to their thermodynamic limits simultaneously without compromising on the charge collection efficiency. The J_{SC} could be improved by harnessing more solar photons, which depends on the bandgap of the light absorber layer. On the other hand, V_{OC} exhibits a strong dependence on the emission characteristics, including emission quantum yield, and charge-carrier recombination dynamics, and FF is primarily influenced by the series resistance and the ideality factor.

In particular, high absorption coefficient[48], high emission quantum yield[49] and long charge-carrier lifetimes[50,51] are essential to maximize the performance, achieved primarily as a result of modification of device arichtecture[52,53], csompositional[54] and solvent engineering[55] in different PSC architectures. As illustrated above, the optoelectronic properties could be tailored by introducing an optimized amount of monovalent metal halide additives into the perovskite precursor solutions. For example, conversion of PbI_2 to $MAPbI_3$ can be improved by adding MI (M = Na, Ag, and Cu) additives. The devices were fabricated using FTO/compact-TiO_2/mesoporous-TiO_2/$MAPbI_3$/Spiro-MeOTAD/Au architecture, and were examined under simulated air mass 1.5 global (AM1.5G) solar irradiation. The current density–voltage (JV) characteristics as presented in Figure 8a of the pristine- and MI-based perovskite devices demonstrated improvement in the power conversion efficiency. A relatively smaller cation, i.e., Na^+ increased the J_{SC} by 2 mA/cm^2, and FF from 70 to 73%, leading to an overall enhancement in the PCE to 15% (PCE of control devices = 14%). This gain in output power is realized at the expense of 50 mV drop in V_{OC}, which occurred due to the presence of undesired contacts associated with relatively high roughness of perovskite films[9].

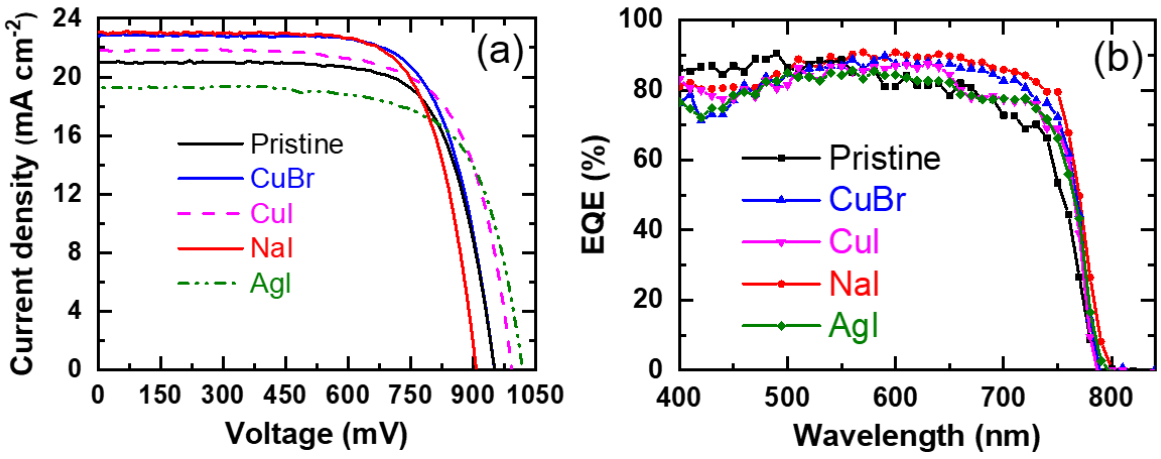

Figure 8: Photovoltaic performance of solar cells containing NaI, AgI, CuI and CuBr based $MAPbI_3$ films. (a) JV data recorded under standard illumination and (b) EQE as a function of illumination wavelength[9].

In contrast, AgI introduction increased the photovoltage significantly by 100 mV, and improved the FF by balancing the charge transport behavior, however, a significant drop in the photocurrent density marginally improved the overall performance of the device. Employing CuI additive rendered the $MAPbI_3$ films smooth and contiguous, which translated into better photovoltaic parameters including J_{SC}, V_{OC} and FF. By changing the source of Cu^+ to CuBr, P_{out} of 15.6% was obtained, primarily due to high photocurrent density approaching 23 mA/cm^2. Furthermore, the enhancement in photocurrent densities, when NaI-, CuI-, and CuBr-based perovskite films are used as a light absorber, is greatly supported by external quantum efficiency (EQE) data shown in Figure 8b. EQE as a function of illumination wavelength brought out that these additives do not alter the bandgap of the $MAPbI_3$ as the generation of photocurrents begins at around 780 nm irrespective of the monovalent metal cation[9].

In addition to Na^+, relatively larger alkali cations including rubidium (Rb) and potassium (K) have been explored as a monovalent metal halide additive to improve the power conversion efficiencies. Rb^+ was initially reported to be incorporated in the perovskite structures[22], however, structural studies established that Rb^+ is too small to occupy the A-site in the 3D $MPbX_3$ lattice[56,57]. The influence of Rb^+ as a monovalent additive cation on the performance of perovskite solar cells was further explored as shown in Figure 9. This study showed that RbI incorporation into the precursor solution increased the open-circuit voltage of the device by

100 mV, leading the realization of V_{OC} as high as 1.23 V under standard illumination conditions Figure 9b.

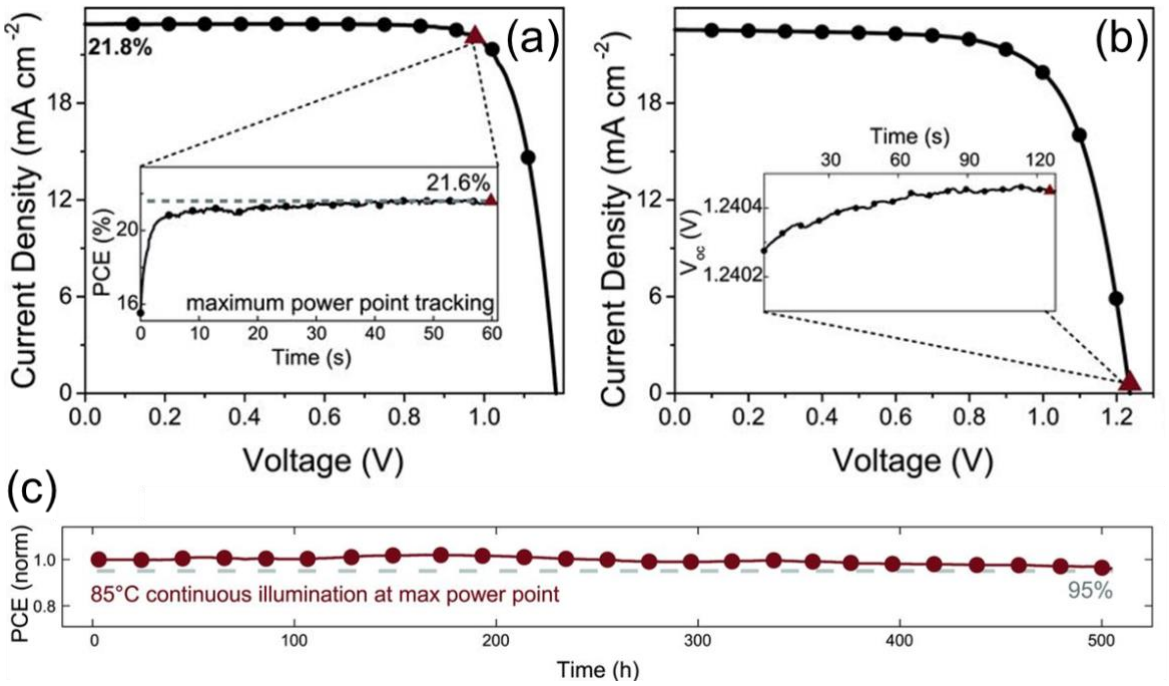

Figure 9. Photovoltaic performance of solar cells containing RbI based perovskite films. (a) Current density–voltage (JV) curve, taken at 10 mV s^{-1} scan rate, of the solar cell with 21.8% efficiency (V_{oc} = 1180 mV, J_{sc} = 22.8 mA cm^{-2}, and FF = 81%). The inset shows the scan rate–independent MPP tracking for 60 s, resulting in a stabilized efficiency of 21.6% at 977 mV and 22.1 mA cm^{-2} (displayed as triangles in the J-V and MPP scans). (b) J-V curve of the highest-V_{oc} device. The inset shows the V_{oc} over 120 s, resulting in 1240 mV (displayed as the red triangles in the J-V and Voc scans). (c) Operational stability under full-sun illumination at 85-degree centigrade recorded for the perovskite solar cell containing RbI additive.

This highlights a powerful design strategy for high V_{OC} and more effective charge extraction in PSCs through energy level engineering of the interfaces. A general comparison establishes that remarkable V_{OC} is a key photovoltaic metric that distinguishes PSCs from other photovoltaic technologies. Therefore, a high degree of interest focussing V_{OC} has emerged in PSCs involving application of various additive-based light absorbers, and impressive progress has been made especially in terms of V_{OC}, which has reached an unprecedented mark of 1.26 V. Besides high V_{OC}, the RbI-based device yield high *FF* value. Electrochemical Impedance and other electrical characterization techniques revealed the improvement of charge transport across the interfaces on either side of RbI-based perovskite absorber layer[22]. In summary, this combination of small perturbation techniques, including intensity-modulated photocurrent

spectroscopy (IMPS) and intensity-modulated photovoltage spectroscopy (IMVS) revealed that Rb incorporated PSCs show faster photocurrent transient response, enhanced charge transport, slower charge-carrier recombination, and less capacitance[22,57].

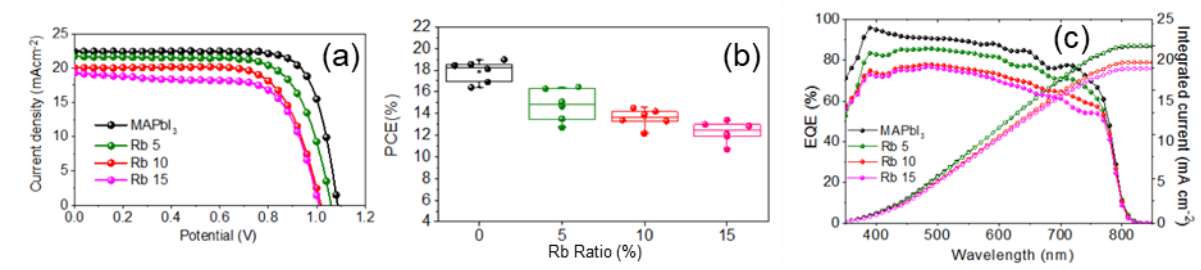

Figure 10. Photovoltaic performance of solar cells containing RbI based $MAPbI_3$ films. (a) JV data recorded under standard illumination, (b) the extracted PCE values showing the dependence of efficiency on RbI concentration and (c) EQE as a function of illumination wavelength[58].

To understand the role of Rb^+, a controlled experiment involving mixing of RbI and MAPbI3 was undertaken, and the photocurrent density-voltage (*J-V*) (Figure 10a) measurements were carried out on the devices involving $MAPbI_3$, and $Rb_xMA_{1-x}PbI_3$ perovskite films. The performance decreased from 19.0% to 13.4% and V_{OC} decreased from 1086 mV for $MAPbI_3$ to 1010 mV by introducing 15% RbI into the solution, i.e., when $Rb_{0.15}MA_{1-0.15}PbI_3$ films are used as the light absorbers (Figure 10b). The undesired formation of pinholes and the occurrence of increased parasitic non-radiative recombinations in the $Rb_xMA_{1-x}PbI_3$ films could explain the drop in the photovoltaic performance of the devices. The $MAPbI_3$ perovskite band edge remains unchanged with increasing Rb^+ content from 5 to 15%, as the external quantum efficiency (EQE) (Figure 10c) recorded by monitoring the short-circuit current at different incident wavelengths revealed that the photocurrent generation begins at around the same incident wavelength irrespective of the composition[58].

Given the remarkable photovoltaic performances obtained from judiciously optimized perovskite composition containing RbI, rational studies were carried by choosing mixed-halide ($MAPb(I_{0.85}Br_{0.15})_3$), and mixed-cation ($FA_{0.85}MA_{0.15}PbI_3$) systems. The devices with normal architecture fabricated using $Rb_xMA_{1-x}Pb(I_{0.85}Br_{0.15})_3$ and $Rb_x(FA_{0.85}MA_{0.15})_{1-x}PbI_3$ films amply established that the presence of Rb^+ has a detrimental effect on the power conversion efficiency of the solar cell. The EQE spectra recorded for the devices involving Rb-based absorbers, i.e., $Rb_xMA_{1-x}Pb(I_{0.85}Br_{0.15})_3$ and $Rb_x(FA_{0.85}MA_{0.15})_{1-x}PbI_3$ rule out the incorporation

of Rb^+ in these 3D perovskite lattices as the current generation as a function of illumination wavelength starts at the same wavelength[57].

In a similar direction, careful studies revealed that monovalent halides based on K^+ can influence various photovoltaic parameters. For example, the introduction of KI into $(Cs_{0.06}FA_{0.79}MA_{0.15})Pb(I_{0.85}Br_{0.15})_3$, a state-of-the-art triple-cation perovskite composition, greatly improved the external photoluminescence quantum yields, with internal yields exceeding 95 %. This consequently improved the open-circuit voltage from 1.05 to 1.17 V, and FF from 73% to 79%, which translate into PCEs greater than 21%[33]. As compared to Rb^+ incorporation, K+ seems to exhibit a profound effect on the luminescence owing to it's a relatively higher tolerance limit for the triple-cation perovskites, and structural and elemental analyses revealed that Rb^+ exhibits a selective affinity towards iodide whereas K^+ binds to bromide[44].

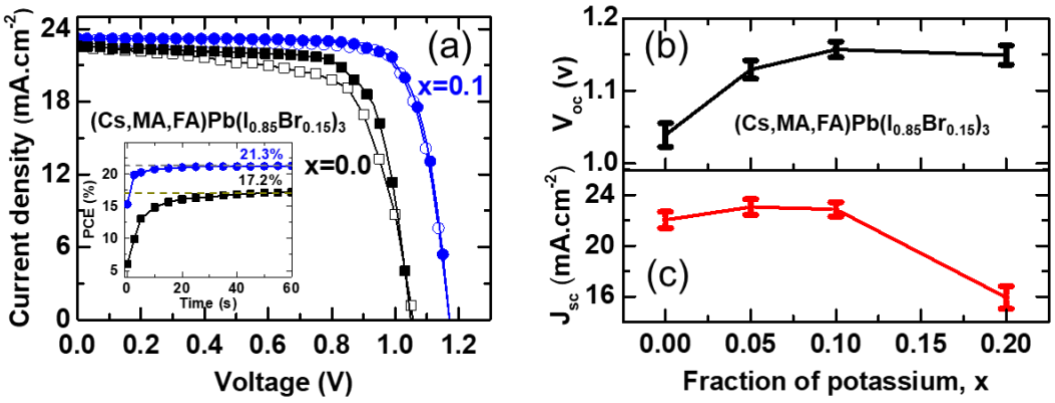

Figure 11. Photovoltaic performance of solar cells containing KI based perovskite films. (a) Forward (open symbols) and reverse (closed symbols) JVcurves of the best-performing solar cells with $(Cs_{0.06}FA_{0.79}MA_{0.15})Pb(I_{0.85}Br_{0.15})_3$ absorbers without (x=0) and with (x=0.1) KI, measured under AM1.5, 100mW cm^{-2}. Inset, stabilized power output under the same conditions. (b) Open-circuit voltage (VOC) and (c) short-circuit current density (JSC) as functions of potassium fraction x, with error bars representing the standard deviation across ten devices for each composition[33].

It is worth emphasizing that a particular challenge encountered while exploring the full potential of perovskite devices is to understand the origin of degradation and nature of parasitic recombination processes[59,60], which adversely affect the device stability, dynamics and diffusion of charge carriers and in turn, increase the V_{OC} deficit in PSCs[61]. The nature and origin

of traps, which induce non-radiative recombinations, seem to be predominantly associated with the halide vacancies[62]. By introducing an excess amount of monovalent cation-based halides such as KI and RbI, the density of traps or defects could be minimized[34]. In addition to power conversion efficiency, the monovalent metal cations were also probed for their impact on the stability of perovskite solar cells.

For example, RbI was found to greatly improve the operational stability of solar cells containing $(Cs_{0.06}FA_{0.79}MA_{0.15})Pb(I_{0.85}Br_{0.15})_3$ based light absorber layer. These measurements were carried out at the maximum output power under continuous illumination at 85-degree centigrade (**Figure 9c)**. Various investigations brought out that KI-treatment greatly mitigates the photoinduced phase segregation in mixed-halide perovskites, which consequently improved the device stability under different stresses[10,33]. Fundamentally, it is not possible to have water or moisture resistant perovskite film or fully assembled device, primarily because of the ionic nature of metal halide perovskites. By decorating these perovskite structures or films with hydrophobic or less reactive species without compromising on the charge transport properties could render these perovskite systems immune towards moisture. Given the fact, these perovskite solar cells will be sealed for large-scale deployment, obtaining operationally stable devices under inert conditions in the laboratory could be sufficient to provide the proof of concept. However, photo- and thermal-induced degradation occurring in the sealed perovskite devices arising from the ion migration within the bulk of perovskite layer, chemical instability of interfaces and charge selective contacts. These monovalent metal halides greatly minimize these detrimental processes and consequently improve the overall stability of the devices.

6. References

1. Bai, S. *et al.* Planar perovskite solar cells with long-term stability using ionic liquid additives. *Nature* (2019) doi:10.1038/s41586-019-1357-2.

2. Kim, D. *et al.* Efficient, stable silicon tandem cells enabled by anion-engineered wide-bandgap perovskites. *Science (80-.).* (2020) doi:10.1126/science.aba3433.

3. Ban, M. *et al.* Solution-processed perovskite light emitting diodes with efficiency exceeding 15% through additive-controlled nanostructure tailoring. *Nat. Commun.* (2018) doi:10.1038/s41467-018-06425-5.

4. Lin, K. *et al.* Perovskite light-emitting diodes with external quantum efficiency exceeding 20 per cent. *Nature* (2018) doi:10.1038/s41586-018-0575-3.

5. Senanayak, S. P. *et al.* A general approach for hysteresis-free, operationally stable metal halide perovskite field-effect transistors. *Sci. Adv.* (2020) doi:10.1126/sciadv.aaz4948.

6. Basiricò, L. *et al.* Detection of X-Rays by Solution-Processed Cesium-Containing Mixed Triple Cation Perovskite Thin Films. *Adv. Funct. Mater.* (2019) doi:10.1002/adfm.201902346.

7. Li, Z. *et al.* Scalable fabrication of perovskite solar cells. *Nature Reviews Materials* (2018) doi:10.1038/natrevmats.2018.17.

8. Tennyson, E. M., Doherty, T. A. S. & Stranks, S. D. Heterogeneity at multiple length scales in halide perovskite semiconductors. *Nature Reviews Materials* (2019) doi:10.1038/s41578-019-0125-0.

9. Abdi-Jalebi, M. *et al.* Impact of Monovalent Cation Halide Additives on the Structural and Optoelectronic Properties of CH 3 NH 3 PbI 3 Perovskite. *Adv. Energy Mater.* **6**, 1502472 (2016).

10. Son, D.-Y. *et al.* Universal Approach toward Hysteresis−Free Perovskite Solar Cell via Defect Engineering. *J. Am. Chem. Soc.* jacs.7b10430 (2018) doi:10.1021/jacs.7b10430.

11. Han, J. *et al.* Hybrid PbS Quantum-Dot-in-Perovskite for High-Efficiency Perovskite Solar Cell. *Small* (2018) doi:10.1002/smll.201801016.

12. McMeekin, D. P. *et al.* A mixed-cation lead mixed-halide perovskite absorber for tandem solar cells. *Science (80-.).* **351**, 151–155 (2016).

13. Azam, M. *et al.* The Positive Function of Incorporation of Small Molecules into Perovskite Materials for High-Efficient Stable Solar Cells. *Sol. RRL* (2019) doi:10.1002/solr.201800327.

14. Lin, Y. *et al.* A piperidinium salt stabilizes efficient metal-halide perovskite solar cells. *Science (80-.).* **369**, 96–102 (2020).

15. Han, T. H. *et al.* Perovskite-polymer composite cross-linker approach for highly-stable and efficient perovskite solar cells. *Nat. Commun.* (2019) doi:10.1038/s41467-019-08455-z.

16. Xu, J. *et al.* Perovskite-fullerene hybrid materials suppress hysteresis in planar diodes. *Nat. Commun.* (2015) doi:10.1038/ncomms8081.

17. Turren-Cruz, S. H., Hagfeldt, A. & Saliba, M. Methylammonium-free, high-performance, and stable perovskite solar cells on a planar architecture. *Science (80-.).* (2018) doi:10.1126/science.aat3583.

18. Abdi-Jalebi, M. *et al.* Monovalent Cation Doping of $CH_3NH_3PbI_3$ for Efficient Perovskite Solar Cells. *J. Vis. Exp.* **J. Vis. Ex**, (2017).

19. Mir, W. J., Sheikh, T., Arfin, H., Xia, Z. & Nag, A. Lanthanide doping in metal halide

perovskite nanocrystals: spectral shifting, quantum cutting and optoelectronic applications. *NPG Asia Materials* (2020) doi:10.1038/s41427-019-0192-0.

20. Saliba, M. *et al.* Cesium-containing Triple Cation Perovskite Solar Cells: Improved Stability, Reproducibility and High Efficiency. *Energy Environ. Sci.* **9**, (2016).

21. Andaji-Garmaroudi, Z. *et al.* A Highly Emissive Surface Layer in Mixed-Halide Multication Perovskites. *Adv. Mater.* (2019) doi:10.1002/adma.201902374.

22. Saliba, M. *et al.* Incorporation of rubidium cations into perovskite solar cells improves photovoltaic performance. *Science (80-.).* **354**, 206–209 (2016).

23. Bowman, A. R. *et al.* Microsecond Carrier Lifetimes, Controlled p-Doping, and Enhanced Air Stability in Low-Bandgap Metal Halide Perovskites. *ACS Energy Lett.* (2019) doi:10.1021/acsenergylett.9b01446.

24. Gong, J. *et al.* Divalent anionic doping in perovskite solar cells for enhanced chemical stability. *Adv. Mater.* (2018) doi:10.1002/adma.201800973.

25. Wang, K. *et al.* Metal Cations in Efficient Perovskite Solar Cells: Progress and Perspective. *Adv. Mater.* (2019) doi:10.1002/adma.201902037.

26. Abdi-Jalebi, M. *et al.* Dedoping of Lead Halide Perovskites Incorporating Monovalent Cations. *ACS Nano* **12**, 7301–7311 (2018).

27. Zhao, W., Yao, Z., Yu, F., Yang, D. & Liu, S. F. Alkali Metal Doping for Improved CH3NH3PbI3 Perovskite Solar Cells. *Adv. Sci.* (2018) doi:10.1002/advs.201700131.

28. Shahbazi, S. *et al.* Ag Doping of Organometal Lead Halide Perovskites: Morphology Modification and p-Type Character. *J. Phys. Chem. C* **121**, 3673–3679 (2017).

29. Bi, C. *et al.* Thermally Stable Copper(II)-Doped Cesium Lead Halide Perovskite Quantum Dots with Strong Blue Emission. *J. Phys. Chem. Lett.* **10**, 943–952 (2019).

30. Son, D.-Y. *et al.* Universal Approach toward Hysteresis−Free Perovskite Solar Cell via Defect Engineering. *J. Am. Chem. Soc.* jacs.7b10430 (2018) doi:10.1021/jacs.7b10430.

31. Lee, J. W. *et al.* Formamidinium and cesium hybridization for photo- and moisture-stable perovskite solar cell. *Adv. Energy Mater.* (2015) doi:10.1002/aenm.201501310.

32. Feldmann, S. *et al.* Photodoping through local charge carrier accumulation in alloyed hybrid perovskites for highly efficient luminescence. *Nat. Photonics* (2020) doi:10.1038/s41566-019-0546-8.

33. Abdi-Jalebi, M. *et al.* Maximizing and stabilizing luminescence from halide perovskites with potassium passivation. *Nature* **555**, 497–501 (2018).

34. Jalebi, M. A. Chemical Modifications and Passivation Approaches in Metal Halide Perovskite Solar Cells. (2018). doi:https://doi.org/10.17863/CAM.30584.

35. Tailor, N. K. *et al.* Recent progress in morphology optimization in perovskite solar cell. *J. Mater. Chem. A* (2020) doi:10.1039/D0TA00143K.

36. Chen, Y. *et al.* Impacts of alkaline on the defects property and crystallization kinetics in perovskite solar cells. *Nat. Commun.* (2019) doi:10.1038/s41467-019-09093-1.

37. Guo, D., Andaji Garmaroudi, Z., Abdi-Jalebi, M., Stranks, S. D. & Savenije, T. J. Reversible Removal of Intermixed Shallow States by Light Soaking in Multication Mixed Halide Perovskite Films. *ACS Energy Lett.* (2019) doi:10.1021/acsenergylett.9b01726.

38. Liu, C., Cheng, Y. B. & Ge, Z. Understanding of perovskite crystal growth and film formation in scalable deposition processes. *Chemical Society Reviews* (2020) doi:10.1039/c9cs00711c.

39. Nie, W. *et al.* High-efficiency solution-processed perovskite solar cells with millimeter-scale grains. *Science (80-.).* **347**, 522–525 (2015).

40. Dar, M. I., Abdi-Jalebi, M., Arora, N., Grätzel, M. & Nazeeruddin, M. K. Growth Engineering of CH 3 NH 3 PbI 3 Structures for High-Efficiency Solar Cells. *Adv. Energy Mater.* **6**, 1501358 (2016).

41. Tang, Z. *et al.* Modulations of various alkali metal cations on organometal halide perovskites and their influence on photovoltaic performance. *Nano Energy* (2018) doi:10.1016/j.nanoen.2017.12.047.

42. Zheng, F. *et al.* Triggering the Passivation Effect of Potassium Doping in Mixed-Cation Mixed-Halide Perovskite by Light Illumination. *Adv. Energy Mater.* (2019) doi:10.1002/aenm.201901016.

43. Cacovich, S. *et al.* Unveiling the Chemical Composition of Halide Perovskite Films Using Multivariate Statistical Analyses. *ACS Appl. Energy Mater.* (2018) doi:10.1021/acsaem.8b01622.

44. Abdi-Jalebi, M. *et al.* Potassium-and rubidium-passivated alloyed perovskite films: Optoelectronic properties and moisture stability. *ACS Energy Lett.* (2018) doi:10.1021/acsenergylett.8b01504.

45. Zhang, R. *et al.* A potassium thiocyanate additive for hysteresis elimination in highly efficient perovskite solar cells. *Inorg. Chem. Front.* (2019) doi:10.1039/c8qi01020j.

46. Nam, J. K. *et al.* Potassium Incorporation for Enhanced Performance and Stability of Fully Inorganic Cesium Lead Halide Perovskite Solar Cells. *Nano Lett.* **17**, 2028–2033 (2017).

47. Kim, S. G. *et al.* Potassium ions as a kinetic controller in ionic double layers for hysteresis-free perovskite solar cells. *J. Mater. Chem. A* (2019) doi:10.1039/c9ta07595j.

48. Abdi-Jalebi, M., Ibrahim Dar, M., Sadhanala, A., Johansson, E. M. J. & Pazoki, M. Optical absorption and photoluminescence spectroscopy. in *Characterization Techniques for Perovskite Solar Cell Materials* 49–79 (Elsevier, 2020). doi:10.1016/B978-0-12-814727-6.00003-7.

49. Richter, J. M. *et al.* Enhancing photoluminescence yields in lead halide perovskites by photon recycling and light out-coupling. *Nat. Commun.* **7**, 13941 (2016).

50. Longo, G. *et al.* Understanding the Performance-Limiting Factors of Cs 2 AgBiBr 6 Double-Perovskite Solar Cells . *ACS Energy Lett.* (2020) doi:10.1021/acsenergylett.0c01020.

51. Doherty, T. A. S. *et al.* Performance-limiting nanoscale trap clusters at grain junctions in halide perovskites. *Nature* (2020) doi:10.1038/s41586-020-2184-1.

52. Pazos-Outon, L. M. *et al.* Photon recycling in lead iodide perovskite solar cells. *Science (80-.).* **351**, 1430–1433 (2016).

53. Friend, R. H., Deschler, F., Pazos-Outón, L. M., Abdi-Jalebi, M. & Alsari, M. Back-Contact Perovskite Solar Cells. *Sci. Video Protoc.* **1**, 1–10 (2019).

54. Merdasa, A. *et al.* Impact of Excess Lead Iodide on the Recombination Kinetics in Metal Halide Perovskites. *ACS Energy Lett.* (2019) doi:10.1021/acsenergylett.9b00774.

55. Jeon, N. J. *et al.* Solvent engineering for high-performance inorganic?organic hybrid perovskite solar cells. *Nat. Mater.* **13**, 897–903 (2014).

56. Kubicki, D. J. *et al.* Phase Segregation in Cs-, Rb- and K-Doped Mixed-Cation (MA) x (FA) 1– x PbI 3 Hybrid Perovskites from Solid-State NMR. *J. Am. Chem. Soc.* **139**, 14173–14180 (2017).

57. Yadav, P. *et al.* The Role of Rubidium in Multiple-Cation-Based High-Efficiency Perovskite Solar Cells. *Adv. Mater.* **29**, (2017).

58. Uchida, R. *et al.* Insights about the Absence of Rb Cation from the 3D Perovskite Lattice: Effect on the Structural, Morphological, and Photophysical Properties and Photovoltaic Performance. *Small* (2018) doi:10.1002/smll.201802033.

59. Abdi-Jalebi, M. *et al.* Charge extraction via graded doping of hole transport layers gives highly luminescent and stable metal halide perovskite devices. *Sci. Adv.* (2019) doi:10.1126/sciadv.aav2012.

60. Stavrakas, C. *et al.* Probing buried recombination pathways in perovskite structures using 3D photoluminescence tomography. *Energy Environ. Sci.* (2018) doi:10.1039/c8ee00928g.

61. Zhao, B. *et al.* High Open-Circuit Voltages in Tin-Rich Low-Bandgap Perovskite-Based Planar Heterojunction Photovoltaics. *Adv. Mater.* **29**, 1604744 (2017).

62. Jones, T. W. *et al.* Lattice strain causes non-radiative losses in halide perovskites. *Energy Environ. Sci.* (2019) doi:10.1039/c8ee02751j.